# Beam time request for E12-10-006: Target Single Spin Asymmetry in Semi-Inclusive Deep-Inelastic $(e, e'\pi^{\pm})$ Reaction on a Transversely Polarized $^3$He Target at 8.8 and 11 GeV

July 1, 2011


Spokerspersons: J.P. Chen[1], H. Gao [2] (contact), X.D. Jiang[3], J.C. Peng[4], X. Qian[4]

[1] *Jefferson Lab, Newport News, VA*

[2] *Duke University and TUNL, Durham, NC*

[3] *Los Alamos National Laboratory, Los Alamos, NM*

[4] *University of Illinois, Urbana-Champaign, IL*

[5] *California Institute of Technology, Pasadena, CA*

**the E12-10-006 Collaboration [1] and the HallA Collaboration**



### Abstract

We propose to carry out precision measurements of Single target Spin Asymmetries (SSA) from semi-inclusive electroproduction of charged pions from a 40-cm long transversely polarized $^3$He target in Deep-Inelastic-Scattering kinematics using 11 and 8.8 GeV electron beams. We propose to carry out this coincidence experiment in Hall A with a newly proposed solenoid spectrometer (SoLID) and the standard Hall A polarized $^3$He target. The full $2\pi$ azimuthal angular coverage on the $\phi_S$ angle and large azimuthal angular coverage on the $\phi_h$ angle are essential in controlling the systematic uncertainties in extracting different asymmetries. The proposed experiment will provide precise 4-D ($x$, $z$, $P_T$ and $Q^2$) data on the Collins, Sivers and Pretzelosity asymmetries for the neutron through the azimuthal angular dependence. The results from this experiment, when combined with the future proton Collins asymmetry measurement and the Collins fragmentation function determined from the $e^+e^-$ collision data, will allow for a flavor separation of the quark tensor charge, and achieve a determination of the tensor charge of d quark to better than 10%. The extracted Sivers and Pretzelosity asymmetry will provide important information to understand the correlation between the quark orbital angular momentum and the nucleon spin. We request a total of 90 days of beam time (polarized) at incident beam energies of 11 and 8.8 GeV and at a beam current of 15 $\mu$A.


[1] E12-10-006 collaboration list can be found at `http://www.tunl.duke.edu/~mep/pac38/update/E12_10_006_Collaboration.pdf`

# 1 Introduction

This document is a brief update to experiment E12-10-006 [1], which is an update to proposal PR12-09-014 [2], on measurements of Target Single Spin Asymmetry (TSSA) in semi-inclusive deep-inelastic $(e, e'\pi^{\pm})$ reaction on a transversely polarized $^3$He target at 8.8 and 11 GeV. The experiment was approved by PAC35. The d quark tensor charge determined from this experiment will provide an important test of lattice QCD predictions for this fundamental quantity. The extracted Sivers and pretzelosity asymmetry will provide important information to understand the correlation between the quark orbital angular momentum and the nucleon/quark spin.

# 2 Motivation

In recent years, the hadronic physics community has extended its investigation of partonic structure of hadrons beyond parton distribution functions (PDFs) by exploring the parton's motion in the direction perpendicular to the parent hadron's momentum. Such effort is closely connected to the study and extraction of a new type of parton distributions: the transverse momentum dependent parton distributions (TMDs) [3, 4, 5, 6, 7]. The ultimate knowledge of finding a single parton inside a hadron – involving both momentum and space information – could be encoded in the phase-space distributions of quantum mechanics, such as the Wigner distribution $W(\vec{k}, \vec{b})$, whose integration over the parton spatial dependence $(\vec{b})$ leads to the TMDs. Understanding both the momentum and spatial distribution of a parton inside a hadron in terms of the more general Wigner distributions could be the central object of future studies on partonic structure.

At leading twist there are eight TMD quark distributions [8]: three of them, the unpolarized, the helicity and the transversity distributions, survive in the collinear limit, while the other five vanish in such a limit. Each TMD quark distribution explores one unique feature of the quark inside a polarized or unpolarized nucleon. An intuitive interpretation of the transversity distribution, $h_1$, is that it gives the probability of finding a transversely polarized parton inside a transversely polarized nucleon with certain longitudinal momentum fraction $x$ and certain transverse momentum $k_T$. The Sivers function [4, 9], $f_{1T}^{\perp}$, provides the number density of unpolarized partons inside a transversely polarized proton, while the Boer-Mulders function [7], $h_1^{\perp}$ , gives the number density of transversely polarized quarks inside an unpolarized proton. Both the Sivers function $f_{1T}^{\perp}$ and the Boer Mulders function $h_1^{\perp}$ require wave function components with nonzero orbital angular momentum and thus provide information about the correlation between the quark orbital angular momentum (OAM) and the nucleon/quark spin, respectively. Furthermore, they are (naive) T-odd functions which rely on the final state interactions (FSI) experienced by the active quark in a SIDIS experiment as both functions vanish without FSI. In contrast to $f_{1T}^{\perp}$ and $h_1^{\perp}$, the functions $g_{1T}$ and $h_{1L}^{\perp}$ are (naive) T-even, and thus do not require FSI to be nonzero. Nevertheless, they also require interference between wave function components that differ by one unit of OAM and thus require OAM to be nonzero. Finally, the 'pretzelosity' $h_{1T}^{\perp}$ requires interference between wave function components that differ by two units of OAM (e.g. p-p or s-d interference).

Recently, the first numerical results on $T$-even, "process-independent" TMDs were reported [10, 11] on the lattice. These calculations are performed with the direct, straight gauge link between the quark fields ("process-independent"), as such at the present time they can not be compared with those from experimental mesurements of SIDIS and Drell-Yan processes. However, they represent major advancements in the study of TMD physics. In principle, calculations on the lattice relevant to SIDIS or Drell-Yan processes could be feasible if one can create a staplelike gauge link, and overcome major technical challenges such as handling diminishing signal-to-noise ratios for increasing nucleon momenta and the statistical noise created by the long gauge link. At the DIS2011 workshop, preliminary results on Sivers and Boer-Mulders functions were reported [12] using a staplelike gauge link.

Although explicit gluon degrees of freedom are lacking in quark models, major progresses have been made utilizing quark models in gaining insight about TMDs and providing tools for analyzing SIDIS and Drell-Yan data in a phenomenolgical way. We discuss briefly few of them. Recently, Avakian *et al.* [13] reported a study of six leading- and eight subleading-twist TMDs (14 $T-$ even TMDs in total) in the bag model and showed that there are 9 linear and 2 nonlinear relations among these TMDs. One of those linear relations connects the moment of pretzelosiy to the difference of $g_1^q$ and $h_1^q$. Such a difference between the helicity and transversity distributions is found to be related to quark orbital angular momentum (OAM) in a light-cone SU(6) quark-diquark model [14], and provides a connection of pretzelosity distribution to OAM in a model dependent way beyond the intuitive picture that TMDs are connected to OAM. This finding also agrees with that from a light-cone SU(6) quark-diquark model [15] at leading twist.

Most recently, five-dimensional Wigner functions in transverse position and three-momentum of the quark relative to the nucleon are studied [16]. The Wigner functions are obtained by Fourier transform in the transverse space of the generalized transverse-momentum dependent parton distributions. Quark OAMs are then calculated using these Wiger functions within different light-cone quark models and the results are compared to different definitions of OAM using generalized parton distributions and TMDs. The sum of quark OAM integrated over $x$ is found to be the same using all three definitions.

All eight leading twist TMDs can be accessed in SIDIS. Four of them (transversity, sivers, pretzelosity and $g_{1T}$) can be accessed through a transversely polarized target. In this approved experiment, we will measure precisely in 4-D space the Collins, Sivers asymmetry, and the pretzelosity asymmetries. The recent discovery of a "sign mismatch" [17] between the Sivers function and the corresponding twist-three quark-gluon correlation function $T_{q,F}(x,x)$ extracted from SIDIS and single hadron production from $pp$ collision highlights further the importance of this experiment. For details about the formalism on SIDIS differential cross sections and SSA, we refer to our original PAC34 proposal [2].

# 3 New developments since PAC 35

We present new results from E06-010 first followed by latest updates concerning solenoid magnet options, GEM, cerenkov, and MRPC detectors. Updates on calorimeter, and GEANT 4 simulations can be found in the PAC38 update to the PAC37 approved experiment [18].

## 3.1 New results from E06-010

Complementing the data from the HERMES [19], COMPASS [20], and BELLE [21] experiments, the recent release from the Jefferson Lab HallA experiment E06-010 [22] on the neutron (with polarized $^3$He) will facilitate a flavor decomposition of the transversity distribution function, $h_1$ and the Sivers distribution function $f_{1T}^{\perp}$ in the overlapping kinematic region. The extracted neutron Collins/Sivers moments from [22] are shown in Fig. 1. The Collins moments are compared with the phenomenological fit [23], a light-cone quark model calculation [24, 25] and quark-diquark model [25, 26] calculations. The phenomenological fit and the model calculations, which assume Soffer's bound [27], predict rather small Collins asymmetries which are mostly consistent with

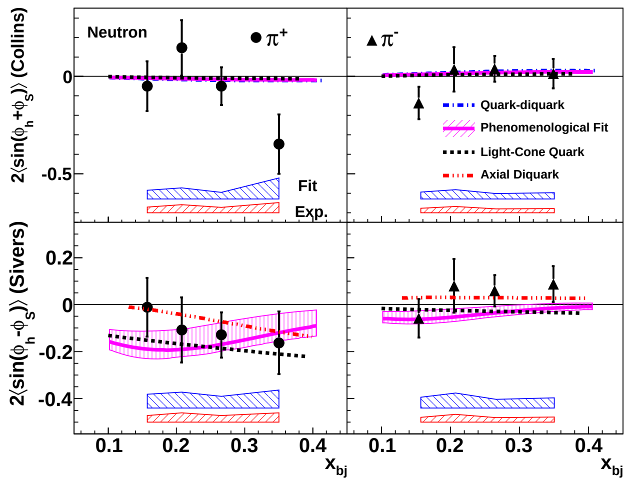


Figure 1: The extracted neutron Collins and Sivers moments with uncertainty bands for both $\pi^+$ and $\pi^-$ electro-production. For details, see Ref. [22].

the data shown in fig. 1. However, the $\pi^+$ Collins moment at $x = 0.35$ is suggestive of a noticeably more negative value at the $2\sigma$ level. These new neutron data favor negative $\pi^+$ Sivers moments, while the $\pi^-$ moments are close to zero. Such behavior independently supports a negative $d$ quark Sivers function, which has been suggested by the phenomenological fit [28, 29] to HERMES and COMPASS data, a light-cone quark model calculation [30, 31], and an axial diquark model calculation[32]. In addition, the central values of these new data are slightly smaller in magnitude than the phenomenological fit. This experiment has demonstrated the power of polarized $^3$He as an effective polarized neutron target, and has laid the foundation for future high-precision measurements of neutron TMDs using a polarized $^3$He target and SoLID following the JLab 12 GeV upgrade.

### 3.2 Magnet feasibility studies

Detailed simulations and projections of this experiment have been carried out previously with the BaBar and CDF magnets. In this section, we present studies on the feasibility of using the ZEUS solenoid magnet and the new Glue-X solenoid magnet in the SoLID-SIDIS experiment. Compared to BaBar and CDF magnets, these two magnets have smaller dimensions but stronger magnetic fields.

A Monte Carlo simulation was done based on GEANT4. We use similar layout in the simulation as previous designs using the BaBar and CDF solenoid magnet. The entire detector system consists of forward angle detectors and large angle detectors. The main purpose is to determine the kinematic coverage and the $p_T$ vs $\phi_h$ coverage at 11 GeV. To achieve this, we put both forward angle and large angle calorimeters in our simulation.

For ZEUS magnet, the forward angle is $7^\circ$-$14^\circ$, and large angle covers $11^\circ$-$18.3^\circ$. Compared with BaBar magnet, we lose 6 degrees at large angle due to the smaller dimensions of the solenoid magnet. The phase space coverage is obtained by uniformly generating electrons and pions into the SoLID. Compared with BaBar, the $x$ coverage is reduced from 0.05-0.65 to 0.05-0.55, the $Q^2$ coverage is 1-6 GeV instead of 1-9 GeV, and $p_T$ coverage is 0-1.45 GeV instead of 0-1.7

GeV. The $p_T$ vs $\phi_h$ coverages for different kinematic bins are also obtained. For the Glue-X magnet, a better kinematic converage is achieved by having both the forward and the large angle calorimeters inside the solenoid with $Q^2 = 1$ - 8 (GeV/c)$^2$, $p_T = 0 - 1.25$ (GeV/c) and $x = 0.05$ - 0.065. When compared with the design using BaBar solenoid magnet [2], the $p_T$ vs $\phi_h$ coverages for both ZEUS and Glue-X are significantly reduced, especially at higher $x$ higher $z$ range. Due to smaller dimensions, a design using solenoid ZEUS or Glue-X would suffer a significant loss of $\phi_h$ coverage at higher $x$ and higher $z$ region, which is very important for SSA experiments; thus renders either one an unsuitable option for the SoLID-SIDIS experiment [2, 1, 18]. Given that the geometry and the field of the CLEO magnet are very similar to those of the BaBar magnet, we conclude that an existing magnet of choice for this experiment will be either one of these three magnets: BaBar, CLEO and CDF.

### 3.3 Update on the GEM detector

The SoLID spectrometer requires high resolution track reconstruction under high rate conditions over a large area. A cost effective solution for large-area tracking in a high-rate environment is provided by the Gas Electron Multiplier (GEM) technology invented by F. Sauli [33] in 1997. The GEM is based on gas avalanche multiplication within small holes (on a scale of 100 $\mu$m), etched in a Kapton foil with a thin layer of copper on both sides. The avalanche is confined in the hole resulting in very fast (about 10 ns rise time) signals. Several GEM foils (amplification stages) can be cascaded to achieve high gain and stability in operation. The relatively small transparency of GEM foils reduces the occurrence of secondary avalanches in cascaded GEM chambers. All these properties result in very high rate capabilities of up to 100 MHz per cm$^2$ and an excellent position resolution of 70 $\mu$m. GEM detectors have also been shown [34] to work very well in a strong perpendicular magnetic field up to 5 Tesla. Triple GEM chambers were successfully used in the COMPASS experiment at CERN [35]. One challenge we are facing for the GEM trackers of SoLID is the large active area required. The back trackers of SoLID need to have circular disk-type GEM chambers extending radially from 1 m to 2.25 m . These areas are significantly large compared to the 32×32 cm$^2$ area of the COMPASS chambers. In the past the maximum GEM foil area had been limited to 45×50 cm$^2$. However, over the last few years the Micro Pattern Gas Detector (MPGD) group at CERN, in collaboration with INFN, has perfected two techniques to produce large area GEM foils: single mask GEM etching and GEM splicing [36, 37]. The single mask technique allows for the fabrication of foils as large as 60×100 cm$^2$. The splicing technique allows for two such foils to be combined with only a 3 mm wide dead zone between the two foils (See Fig 5, right). The MPGD group has already succeeded in producing GEM foils as long as 200 cm and as wide as 50 cm. They are confident that they can fabricate GEM foils as large as 200×100 cm$^2$ within two years using the two new techniques.

This new GEM technology is developed and shared through the CERN RD-51 collaboration (Collaboration for the development of micro-Pattern gas detectors technologies). Four of the groups responsible for GEM chambers of SoLID, CIAE (Li group)), INFN (Cisbani group), UVa (Liyanage group), and USTC (Zhao group) are members of the RD-51 collaboration. The INFN and the UVa groups are also leading an aggressive R&D program to develop large area GEM chambers for the hall A Super-Bigbite apparatus (SBS). The active area of large tracking chambers of SBS will be 50×200 cm$^2$. These large GEM trackers will be assembled by combining five 40×50 cm$^2$ "chamber modules" with narrow edges. The readout of the SBS and SoLID GEM chambers will be based on the APV25-S1 chip [38], currently in use for the COMPASS GEM trackers and the CMS silicon strip detectors.

The UVa and INFN groups successfully constructed and instrumented a prototype tracking telescope consisting of five 10 cm × 10 cm GEM chambers. This tracker was installed on hall A left high resolution spectrometer for the PREX experiment. The GEM chambers worked well under very high rate conditions during the experiment yielding a track resolution of $\sim 70\ \mu m$ (Fig 4). The INFN group also constructed a 40×50 cm$^2$ prototype GEM chamber and an APV25-S1 based readout system. We plan to construct a second such prototype at UVa this summer. The UVa group is also purchasing a 2800 channel APV25 based readout system. We are planning a test run with the 10 cm × 10 cm tracker plus the two 40×50 cm$^2$ GEM chambers in hall A during the g2p/gep experiment scheduled for the winter of 2011.

An important issue concerning large GEM chambers is the high capacitance in long readout strips. SoLID requires readout stripes longer than 1 m and stripes longer than 0.5 m have not been used before. We will use the prototype chamber, with multiple readout stripes connected together, to study the impact of high stripe capacitance on resolution and noise. Furthermore, there are several other large area GEM detector projects currently underway around the world [39, 40]. Given this rapid progress towards large area GEM chambers, we do not anticipate any serious technical difficulties facing the fabrication of SoLID GEM trackers.

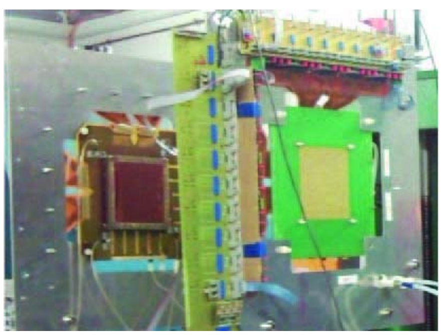

Figure 2: GEM chambers of the prototype tracker being prepared for the beam tests during hall A PREX experiment.

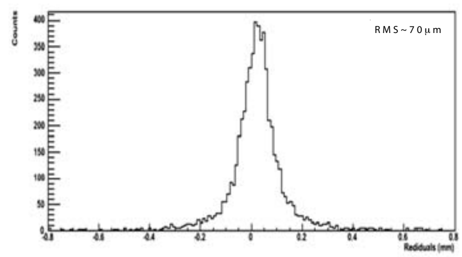


Figure 3: The residual distribution for one GEM projection, showing the high resolution achieved from our prototype GEM chambers.

### 3.4 The Cherenkov Detectors

This experiment requires both electron and pion detection. In order to unambiguously identify both electrons and pions several PID detectors will be required. Two Cherenkov detectors will be an essential part of the PID scheme.

**Electron identification: the light-gas Cherenkov** A Cherenkov detector filled with $CO_2$ at 1 atm would ensure electron-pion separation up to a momentum of 4.65 GeV. This detector, extending 2.1 m along the beam line, would be positioned immediately after the SoLID coil. The close proximity to the SoLID magnet requires careful consideration of various options for the photon detectors. In addition, the detector optical system is expected to provide full coverage in the azimuthal angle.

Recently a GEANT4 simulation was used to optimize the design of the optical system. It was found that with just one system of 30 spherical mirrors (following the SoLID sectoring) near perfect collection efficiency, $> 95\%$, can be achieved with a $12''$ by $12''$ photon detector (active area). This size could be easily scaled down to $6''$ by $6''$ by employing Winston cones.

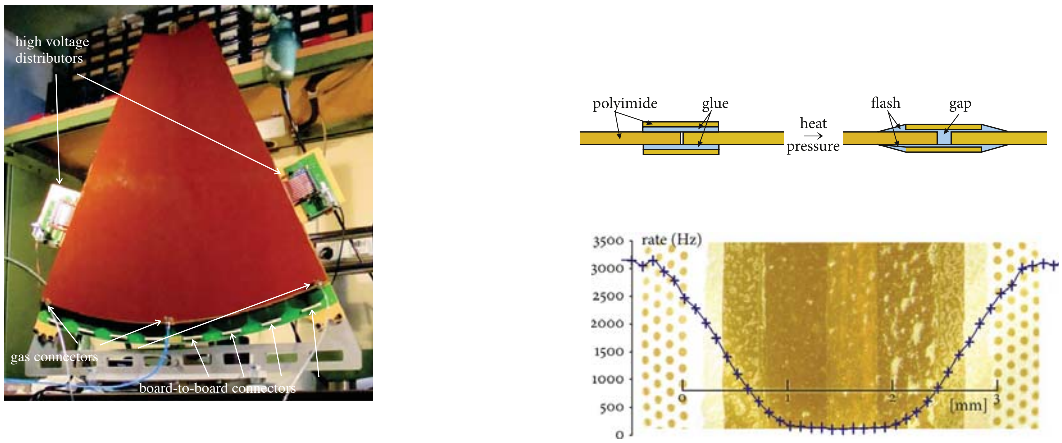


Figure 4: Left: Large area GEM prototype built at CERN for a possible future upgrade of the TOTEM detector. For this chamber 33 cm $\times$ 66 cm GEM foils were spliced together to make 66 cm $\times$ 66 cm foils. Right top: The principle of GEM splicing. Right bottom: Microscope image of the seam and the results of a X-ray scan showing the $\sim$ 3 mm dead-area. (Figures from Rui De Oliveira, 5$^{\text{th}}$ RD51 Collaboration Meeting, Friburg, Germany, May 2010)

A schematic of this setup is shown in Fig. 5 where Cherenkov photons (green) produced by the passage of electrons (red) through the radiator gas are reflected by 30 spherical mirrors (grey) and focused onto the photon detectors (cyan).

The one-mirror optical system is a significant improvement over the three-mirror design outlined in our PAC35 proposal. The Cherenkov photon yield lost due to reflections off multiple mirrors is reduced. This is particularly important for the GEM + CsI option where is technically challenging to manufacture and maintain mirrors with good reflectivity in the UV region. In addition the one-mirror design is more practical and cost efficient form the manufacturing and installation point of view. The same GEANT4 simulation has been used to describe the photon detector response and this is yet another improvement since PAC35. Two options have been considered for the photon detectors: magnetic field resistant photomultiplier tubes, PMTs, (Fig. 5, left panel) to be used in combination with Winston cones and gaseous electron multipliers

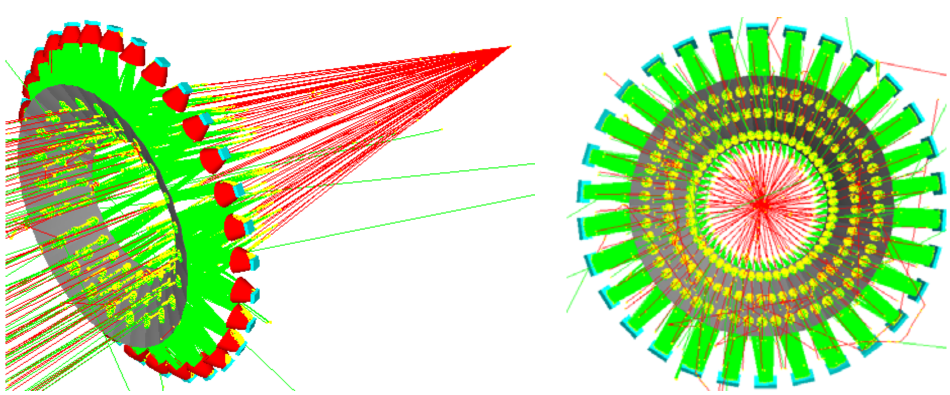

Figure 5: Setup of the light-gas Cherenkov: a system of 30 spherical mirrors (grey) will focus the Cherenkov photons (green) created by the passage of electrons (red) through a radiator gas onto photon detectors (cyan). Left panel: setup for the PMT option, side view (see text). Right panel: setup for the GEM + CsI option, back view - as seen from the beam dump (see text).

with Cesium Iodide coating, GEMs + CsI, (Fig. 5, right panel).

For the PMT option the Hamamatsu model H10966A-100 was considered. This is a 2″ multi-anode PMT with up to 94% photocathode coverage and good quantum efficiency down to wavelengths of 200 nm. These characteristics make this model ideal for tiling and we plan to use 9 such PMTs per sector, in a 3 by 3 array, to cover a 6″ by 6″ area. It is fairly resistant in magnetic field: such unshielded PMT experiences up to 60% gain reduction in 100 Guass field according to data provided by Hamamatsu. This is a significant improvement when compared to a regular 5″ PMT which, if unshielded, would experience a similar gain reduction at only 4 Gauss. To establish whether H10966A-100 could withstand the magnetic field of SoLID we plan to test it with shielding this Summer at Temple University. If the magnetic field test results are satisfactory we plan additional tests at Jefferson Lab to ensure suitability in high-background environment. An estimate of the number of photoelectrons for this option with the configuration described above (Fig. 5, left panel) yields between 25 and 35 photoelectrons. The number depends slightly on the electron polar angle: because of the mirror positioning in the tank electrons with higher polar angles traverse a longer path in the radiator gas than those with lower polar angles. This estimate includes wavelength dependent corrections like mirror and Winston cones reflectivities and the PMTs quantum efficiency as well as an overall correction of 0.8 to account for the reduction in the photocathode effective area as a result of tiling.

The GEM + CsI is an alternative to the PMT option and has the clear advantage of being resistant in magnetic filed. This has been used successfully as a photon detector during PHENIX experiment at BNL in a Hadron Blind Detector [41] and a similar setup is being developed in Japan for use in JPARC experiments [42]. The photon detector consists of three layers of GEMs the first being covered with CsI which acts as a photocathode. The operational regime for CsI is the ultraviolet (UV) region, between 120 and 200 nm [43]. This requires a radiator gas with good transparency in the UV and with very good purity to avoid photon absorption by impurities. Thus for the GEM + CsI option, a suitable gas choice would be $CF_4$ which, unlike $CO_2$, is transmissive between 120 nm and 200 nm [44]. This gas would still give an acceptable threshold for electron-pion separation and it was the gas of choice for the successful PHENIX run. The number of photoelectrons for this option was estimated using the GEANT4 simulation and assuming a 12″ by 12″ photon detector (Fig. 5, right panel). A signal of 20 to 30 photoelectrons was obtained. Wavelength dependent corrections as mirror reflectivity and quantum efficiency of CsI were taken into account as well as an overall correction of 0.54 to account for loss of signal due to gas transparency, reduced photocathode coverage of the GEM (about 20% of the GEM surface is occupied by holes), transport efficiency of avalanche electrons through gas, etc.

**Pion identification: the heavy-gas Cherenkov** A Cherenkov detector filled with $C_4F_{10}$ at 1.5 atm would be placed right after the light-gas Cherenkov to provide pion-proton/kaon separation in a momentum range from 2.2 to 7.6 GeV. A GEANT4 simulation is underway for this detector and the same design ideas and concepts will be used as for the light-gas Cherenkov. Preliminary results from this simulation on the focusing of Cherenkov light with one spherical mirror have been obtained for charged pions. The photon detector size is set to be 12″ by 12″, and the light collection efficiency is found to be very good for the entire kinematic range of interest. Next step will be to reduce the size of the photon detector by using Winston cones while still keeping good collection efficiency. Then the detector signal will be estimated for the two photon detector options described above.

### 3.5 Update on MRPC

A number of MRPC prototypes have been tested successfully by our collaborators at Tsinghua University (TSU) in the last 10 months or so including the most recent test at Rossemdorf using an electron beam. A prototype is curently being built at TSU for SoLID for a beam test in Hall A in the fall of 2011.

# 4 Beam Request and Projections

### 4.1 Beam time request

We request 90 days of total beam time with 15 $\mu$A, 11/8.8 GeV electron beams on a 40-cm long, 10 amgs transversely polarized $^3$He target. 72 days is for beam on the polarized $^3$He target, which is determined by the precision of the Collins asymmetry measurement in order to achieve a 10% measurement of the tensor charge of the d quark. Such a precision is important for testing LQCD predictions of this fundamental quantity. The proposed precision in 4-D binning of our data allows for a more assumption-independent extraction of the Collins, Sivers and pretzelosity TMDs. A total overhead time of 8 days is also requested. This overhead time will be shared among activities such as unpolarized target runs, target spin flip and target polarization measurements, as has been done in the past during other Hall A polarized $^3$He target experiments. Major target related down times can also be arranged to coincide with the scheduled accelerator maintenance activities in order to reduce overhead time. In addition, we request 10 days for a dedicated study/test of the $x - z$ factorization with Hydrogen and Deuterium gas using a reference cell. Although beam polarization is not required for the proposed SSA measurements, we request a polarized beam for a parasitic measurement of the $A_{LT}$ which can be used to access another leading twist distribution, $g_{1T}$.

### 4.2 Projections

The projections combine both 11 GeV data and 8.8 GeV data. The projected results for $\pi^+$ Collins asymmetry at one typical kinematic bin, $0.45 > z > 0.4$, $3 > Q^2 > 2$, i The $x$-axis is $x_{bj}$. The $y$-axis on the left side is $P_T$ which is the transverse momentum. The $y$-axis on the right side shows the scale of the asymmetry. The $y$-position of the projections shows the average $P_T$ value for the corresponding kinematic bin. The statistical uncertainties follow the scale on the right side of $y$-axis. The scale of the theoretical calculations follow the right side $y$-axis. Also shown in the figure are theoretical predictions from Anselmino *et al.* [23], Ma *et al.* [45], Pasquini [24] and Vogelsang and Yuan [46] for the Collins asymmetry. Complete projections for $\pi^+$ ($\pi^-$) Collins/pretzelosity/Sivers asymmetries in terms of 4-D ($x$, $z$, $P_T$ and $Q^2$) kinematic bins can be found at [47], and the kinematic range covered is $8 > Q^2 > 1$, $0.7 > z > 0.3$, 1.6 $> P_T > 0$, and $0.65 > x > 0.05$.

# 5 Relations to other experiments on TMDs

There are two approved SoLID SIDIS experiments on TMD physics using the standard Hall A high-pressure transversely (longitudinally) polarized $^3$He target: E12-10-006 (E12-11-007). The aim of E12-10-006 is a precise measurement of Collins, Sivers and prezelosity asymmetries in a 4-D kinematic space of $(Q^2, z, x, P_T)$ in order to access the transversity, Sivers and the pretzelosity distributions of the neutron. E12-10-006 is complemented by E12-11-007 in which the two additional TMDs, $h_{1L}^{\perp}$ and $g_{1T}$ will be measured with precision on the neutron.

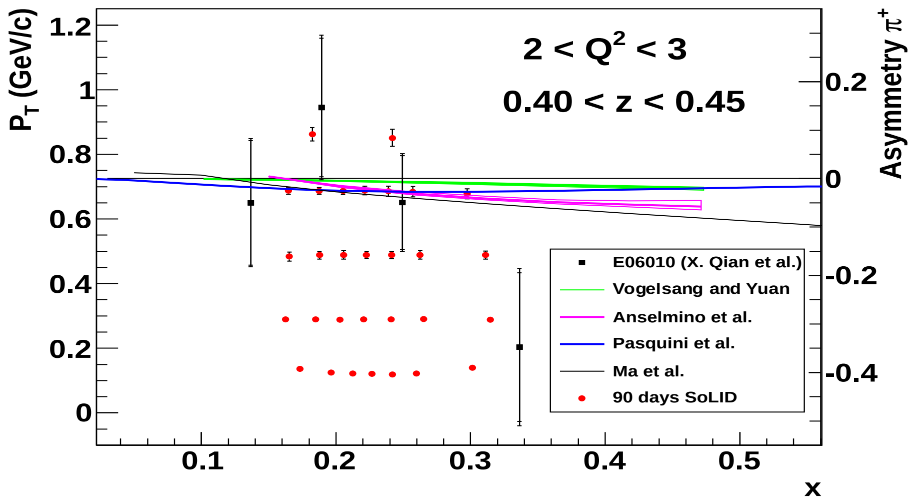


Figure 6: 12 GeV Projections with SoLID and a transversely polarized $^3$He target for $\pi^+$ Collins asymmetries at $0.45 > z > 0.4$, $3 > Q^2 > 2$.

The conditionally approved SIDIS experiment C12-09-018 in Hall A will use the Super-Bigbite spectrometer for detecting mesons and the Bigbite spectrometer for detecting the scattered electrons with an upgraded transversely polarized $^3$He target. A RICH detector (based on the components of the HERMES' RICH is also planned to allow for the identification of kaons in addition to pions). The proposed experiment will provide precise data on the neutron as a function of $x$ and $z$, integrated over $P_T$ and $Q^2$. The experiment proposes two beam energies: 8.8 GeV and 11 GeV in order to have two values of $Q^2$ for each bin of $(x, z)$, and will provide data on neutral pions also.

Hall B has an extensive SIDIS program accessing TMDs. The program includes the approved experiments: E12-06-112, E12-07-107, E12-07-007, E12-09-009 and E12-09-008 using unpolarized and longitudinally polarized proton and deuteron targets. The planned CLAS12 program will also include charged kaon detection using a RICH detector which is anticipated to be added to the CLAS12 detection system. Therefore, the approved CLAS program on TMD physics is completely complementary to our experiment E12-10-006.

## 6 Collaborations

This experiment has a strong collaboration between experimentalists and theorists. It also has a very strong international collaboration with many institutions from Italy and China. A stronger Chinese collaboration has formed since the PAC35 approval of this experiment. The Chinese collaboration has taken on the major responsibilities of the GEM and the MRPC detectors. The Chinese collaboration is also actively applying for fundings from the National Science Foundation of China, Ministry of Science and Technology and Chinese Academy of Sciences.

## References


[1] H. Gao *et al.*, EPJ-plus **126**, 2 (2011); JLab proposal E-12-10-006, PAC35 http://www.jlab.org/exp_prog/proposals/10/PR12-10-006.pdf.

[2] JLab proposal PR-12-09-014, PAC34
http://www.jlab.org/exp_prog/proposals/09/PR12-09-014.pdf.
[3] J.P. Ralston and D. E. Soper, Nucl. Phys. **B152**, 109 (1979).
[4] D.W. Sivers, Phys. Rev. **D41** 83 (1990).
[5] A. Kotzinian, Nucl. Phys. **B441** 234248 1995.
[6] P.J. Mulders and R. D. Tangerman, Nucl. Phys. **B461** 197237 (1996).
[7] D. Boer and P.J. Mulders, Phys. Rev. **D57** 57805786 (1998).
[8] A. Bacchetta et al., JHEP, **02** 093 (2007).
[9] D.W. Sivers, Phys. Rev. **D43** 261-263 (1991).
[10] P. Hägler, B. U. Musch, J.W. Negele, and A. Schäfer, Europhys. Lett. **88** 61001 (2009).
[11] B. U. Musch, P. Hagler, J.W. Negele, and A. Schafer, Phys. Rev. D **83**, 094507 (2011); arXiv:hep-lat/1011.1213 (2010).
[12] B. Musch, https://wiki.bnl.gov/conferences/images/1/1a/Parallel.FD.BernhardMusch.2011-04-14.talk.pdf
[13] H. Avakian, A.V. Efremov, P. Schweitzer and F. Yuan, Phys. Rev. D **81**, 074035 (2010).
[14] B.Q. Ma, and I. Schimidt, Phys. Rev. D **58**, 096008 (1998), B.Q. Ma, I. Schimidt, and J. Soffer, Phys. Lett. B **441**, 461 (1998).
[15] J. She, J. Zhu, and B.Q. Ma, Phys. Rev. **D79** 054008 (2009).
[16] C. Lorce and B. Pasquini, arXiv:1106.0139.
[17] Z.-B. Kang *et al.*, Phys. Rev. D **83**, 094001 (2011).
[18] JLab proposal PR-12-11-007, Spokespersons: J.P. Chen, J, Huang, Y. Qiang, W.-B Yan.
[19] A. Airapetian *et al.* (HERMES), Phys. Rev. Lett. **94**, 012002 (2005), Phys. Rev. Lett.**103** 152002 (2009).
[20] M. Alekseev *et al.*, Phys. Lett. B **673**, 127 (2009).
[21] K. Abe *et al.*, Phys. Rev. Lett. **96**, 232002 (2006).
[22] X. Qian *et al.*, arXiv:1106.0363.
[23] M. Anselmino *et al.*, Phys. Rev. D **75**, 054032 (2007); hep-ph/0701006 (2007).
[24] B. Pasquini, S. Cazzaniga, and S. Boffi, Phys. Rev. **D78** 034025 2008.
[25] S. Boffi, A. V. Efremov, B. Pasquini, and P. Schweitzer, Phys. Rev.**D79** 094012 (2009).
[26] B.Q. Ma, I. Schmidt and J.J. Yang, Phys. Rev. D **65**, 034010 (2002).
[27] J. Soffer, Phys. Rev. Lett. **74**, 1292 (1995).
[28] M. Anselmino *et al.* Phys. Rev. **D72** 094007 (2005).
[29] M. Anselmino *et al.*, arXiv:0812.4366.
[30] S. Arnold *et al.*, arXiv:0805.2137.
[31] B. Pasquini and P. Schweitzer, arXiv:1103.5977.
[32] L.P. Gamberg, G.R. Goldstein and M. Schlegel, Phys. Rev. D **77**, 094016 (2008).
[33] F. Sauli, Nucl. Inst. and Meth. **A386**, 531 (1997).
[34] M. Killenberg *et al.*, Nucl. Instrum. Meth. A **530**, 251 (2004).
[35] B. Ketzer *et al.*, Nucl. Phys. B (Proc. Suppl.) **125**, 368 (2003).
[36] M. Villa, *etal.*, Nucl. Inst. and Meth. **A** (2010), doi:10.1016/j.nima.2010.06.312.
[37] M. alfonsi *et al.*, Nucl. Inst. and Meth. **A617**, 151 (2010).
[38] M.J. French *et al.*, Nucl. Instr. and Meth. A **466** (2001) 359-365.
[39] F. Simon *et al.*, "The Forward GEM Tracker of STAR at RHIC", arXiv:0811.2432v1.
[40] S. D. Pinto, http://www.tunl.duke.edu/~mep/pac38/update/Large-GEM-TOTEM-T1.pdf.
[41] W. Anderson *et al.*, arXiv:1103.4277v1.
[42] K. Auki *et al.*, Nucl. Instr. and Meth. A 628 (2011) 300.
[43] B. Azmoun et al., IEEE Trans. Nucl. Sci. 56-3 (2009) 1544.
[44] C. Lu, K.T. McDonald, Nucl. Instr. and Meth. A343 (1994) 135-151.
[45] J. She and B.Q. Ma, Phys. Rev. D **83**, 037502 (2011).
[46] W. Vogelsang and F. Yuan, *private communications*.
[47] http://www.tunl.duke.edu/~mep/pac38/update/E12-10-006-projection.pdf.